Dynamic memory of a single voltage-gated potassium ion channel: A stochastic nonequilibrium thermodynamic analysis

Kinshuk Banerjee[a)]
Department of Chemistry, University of Calcutta, 92 A.P.C. Road, Kolkata 700 009, India

(Received 7 January 2015; accepted 29 April 2015; published online 8 May 2015)

In this work, we have studied the stochastic response of a single voltage-gated potassium ion channel to a periodic external voltage that keeps the system out-of-equilibrium. The system exhibits memory, resulting from time-dependent driving, that is reflected in terms of dynamic hysteresis in the current-voltage characteristics. The hysteresis loop area has a maximum at some intermediate voltage frequency and disappears in the limits of low and high frequencies. However, the (average) dissipation at long-time limit increases and finally goes to saturation with rising frequency. This raises the question: how diminishing hysteresis can be associated with growing dissipation? To answer this, we have studied the nonequilibrium thermodynamics of the system and analyzed different thermodynamic functions which also exhibit hysteresis. Interestingly, by applying a temporal symmetry analysis in the high-frequency limit, we have analytically shown that hysteresis in some of the periodic responses of the system does *not* vanish. On the contrary, the rates of free energy and internal energy change of the system as well as the rate of dissipative work done on the system show growing hysteresis with frequency. Hence, although the current-voltage hysteresis disappears in the high-frequency limit, the memory of the ion channel is manifested through its specific nonequilibrium thermodynamic responses. © *2015 AIP Publishing LLC.* [http://dx.doi.org/10.1063/1.4920937]

I. INTRODUCTION

Starting from the seminal work of Hodgkin and Huxley,[1] voltage-gated ion channels have attracted considerable attention of experimentalists and theoreticians over the years. This is due to their fundamental role in the creation and propagation of nerve impulse by exchanging ions across the cell membrane.[1–6] The conventional voltage-clamp and patch-clamp techniques have revealed a lot of details of the ion channel kinetics up to the single ion channel level.[4–11] A fascinating feature of ion channels is their bistable behavior reflected in the hysteretic conductance under time-varying voltage showing physiologically functional bio-molecular memory.[12–16] Theoretical analyses have shown that comparable time scales of the external perturbation and system's natural relaxation give rise to such kind of behavior in model systems[17] as well as in ion channels.[18,19] Recently, nonequilibrium response spectroscopic technique[20,21] with periodic voltage protocol is used to study the ion channel kinetics in out-of-equilibrium situations.[22,23] It is obvious that this kind of experimental technique is ideally suited to explore the hysteresis and memory effect in ion channels. A recent study on voltage-gated lysenin channels shows such hysteretic current-voltage characteristics with time-dependent external voltage.[24]

Response of a single ion channel to the external voltage is a stochastic phenomenon with the transition between the channel molecule's different conformational states being random.[18,25] The hysteresis in current-voltage plots is found to be dynamic,[26] which vanishes in the limits of very slow as well as very fast voltage variation, so does the memory that can be measured by the hysteresis loop area.[14,18] Recently, Pustovoit *et al.*[18] have shown that the loop area of the probability-voltage plot tends to zero at very low and very high frequencies of the external voltage. Here, the probability corresponds to the probability of the ion channel to be in the ion-conducting state. This result is very interesting in the context of ion channel memory, and although based on a two-state model, this work provides the basic analytical understanding of channel hysteresis. The time-dependent external voltage keeps the ion channel in a nonequilibrium state,[22] associated with dissipation, that is characterized by a positive value of the total entropy production rate (EPR). Taking an extended version of the ion channel model, it has been found that, although current-voltage as well as total EPR-voltage hysteresis are dynamic in nature, the (average) total EPR increases with voltage frequency to saturation.[27]

With this background in mind, it is therefore natural to ask the questions: (i) how does the vanishing hysteresis correspond with the finite dissipation? and more importantly, (ii) is the vanishing hysteresis in the limiting conditions a general feature, valid for all the periodic responses of the system in the long time limit? To get an understanding of the system's behavior regarding the above issues, various thermodynamic functions are studied using the tools of stochastic nonequilibrium thermodynamics. Interestingly, by employing a temporal symmetry analysis in the high-frequency limit, we analytically show that, instead of diminishing, the hysteresis in some thermodynamic functions grows with voltage frequency. This is verified numerically for the intermediate frequency range.

a)Electronic mail: kbpchem@gmail.com

II. K^+ CHANNEL: STOCHASTIC DESCRIPTION

A potassium ion channel comprises of four independent homologous subunits as affirmed by several experimental studies.[28–30] Each subunit can have various conformational states. For simplicity, here, we consider only two such states—inactive and active.[31,32] Transition between these states is controlled by the external voltage. The state of the channel can be expressed in terms of the number of subunits in active state. The scheme of the voltage-gated channel dynamics is written as

$$\mathrm{C_0} \underset{\mathrm{k_{-1}}(V(t))}{\overset{4\mathrm{k_1}(V(t))}{\rightleftharpoons}} \mathrm{C_1} \underset{2\mathrm{k_{-1}}(V(t))}{\overset{3\mathrm{k_1}(V(t))}{\rightleftharpoons}} \mathrm{C_2} \underset{3\mathrm{k_{-1}}(V(t))}{\overset{2\mathrm{k_1}(V(t))}{\rightleftharpoons}} \mathrm{C_3} \underset{4\mathrm{k_{-1}}(V(t))}{\overset{\mathrm{k_1}(V(t))}{\rightleftharpoons}} \mathrm{C_4}. \quad (1)$$

Here, $\mathrm{C_m}$ represents a state of the ion channel with $m\,(=0, 1, \ldots, 4)$ number of active subunits. m can increase or decrease by one unit due to the occurrence of a forward or a backward reaction having rate constant $k_1(V(t))$ and $k_{-1}(V(t))$, respectively, where $V(t)$ is the time-dependent external voltage. Following Kargol *et al.*,[22] the rate constants are given by

$$k_{\pm 1}(V(t)) = k_{\pm 1}(0) \exp\left(\frac{q_{\pm} V(t)}{k_B T'}\right), \quad (2)$$

where q_+ and q_- are the gating charges associated with each forward and backward transitions, respectively, and $k_{\pm 1}(0)$ are the respective rate constants at zero voltage. T' is the temperature of the environment with which the system is assumed to be in equilibrium and $\mathrm{k_B}$ is the Boltzmann constant. The state $\mathrm{C_4}$, with all the subunits in the active state, is taken as the ion-conducting state.[22,27]

For the dynamics of a single ion channel, the number of subunits in active state, m, is a fluctuating quantity.[33–35] Then, it is appropriate to describe the time evolution of the single channel as a Markov process. The corresponding master equation[36,37] can be written as

$$\dot{P}_m(t) = \sum_{m'} W_{m'm}(V(t)) P_{m'}(t), \quad (3)$$

where $P_m(t)$ is the probability of having m number of subunits in active state at time t and $W_{m'm}(V(t))$ is the transition probability from state-m' to state-m having the property

$$\sum_{m'} W_{m,m'} = 0. \quad (4)$$

The transition probabilities are explicitly defined as

$$W_{m-1,m}(V(t)) = k_1(V(t))(n_T - (m-1))$$

and

$$W_{m+1,m}(V(t)) = k_{-1}(V(t))(m+1). \quad (5)$$

Here, $n_T = 4$ represents the total number of subunits of the ion channel molecule.

From Eq. (3), the probability of the ion-conducting state at time t obeys the following equation of motion:

$$\dot{P}_4(t) = \kappa(V(t)) - K(V(t)) P_4(t), \quad (6)$$

where $\kappa(V(t)) = k_1(V(t))\,[1 - \{P_0(t) + P_1(t) + P_2(t)\}]$ and $K(V(t)) = [k_1(V(t)) + n_T k_{-1}(V(t))]$. The solution of the above equation can be written as

$$P_4(t) = P_4(t_0) \exp\left[-\int_{t_0}^{t} K(t')dt'\right] + \int_{t_0}^{t} \kappa(t') \exp\left[-\int_{t'}^{t} K(t'')dt''\right] dt', \quad (7)$$

where t_0 is the initial time and we have dropped the voltage in the argument of the rate constants for brevity. We take the external voltage to be periodic, $V(t) = V_a \sin\omega t$ with amplitude V_a, frequency $\nu = \omega/2\pi$, and time period T. Now, following Pustovoit *et al.*,[18] the probability in the long-time limit, denoted here with superscript "ss," can be written as[27]

$$P_4^{ss}(t) = \frac{\Delta(t)}{1-\phi}, \quad (8)$$

where

$$\Delta(t) = \int_{t}^{t+T} \kappa(t') \exp\left[-\int_{t'}^{t+T} K(t'')dt''\right] dt' \quad (9)$$

and

$$\phi = \exp\left[-\int_{0}^{T} K(t)dt\right]. \quad (10)$$

From the above expression, the following limiting behaviors can be obtained:[18,27]

$$\begin{aligned} P_4^{\mathrm{ss}}(t) &= \frac{\kappa(t)}{K(t)}, \quad \omega \to 0, \\ P_4^{\mathrm{ss}} &= \frac{\langle \kappa(t) \rangle}{\langle K(t) \rangle}, \quad \omega \to \infty. \end{aligned} \quad (11)$$

So, in the high-frequency limit, P_4^{ss} becomes independent of time. Here, $\langle (\ldots) \rangle = \frac{1}{T}\int_0^T (\ldots) dt$ denotes average over a period T.

III. ION CHANNEL AND MEMRISTOR

Before going to the details of hysteresis in different system properties, let us briefly mention some theoretical ideas and results in the literature regarding the memory effect in ion channels and its connection to electrical circuit elements. The response of the ion channel to external voltage is the experimentally measurable ionic current that can manifest the memory of the channel molecule with time-varying voltage.[24] Long ago, Chua and Kang showed that current-voltage characteristics described by the Hodgkin-Huxley ion channel model follow a set of nonlinear dynamic equations described by them as memristive equations.[38] Memory resistor or memristor was also proposed by Chua earlier as the fourth basic passive circuit element.[39] After decades of search for this element, Strukov *et al.*[40] have recently suggested that memristance occurs naturally in electronic nanodevices. They have presented a model of a semiconductor film composed of variable resistance parts whose sizes are functions of the external voltage and gave an analytical expression for the memristance explaining various switching and hysteretic conductance phenomena in nanoscale devices. Following their approach,[40] here, we write down the

expression of ionic current $I(t)$ of the ion channel molecule as

$$I(t) = [g_{\rm on}(V(t))P_4(t) + g_{\rm off}(V(t))(1 - P_4(t))]\,(V(t) - V_r). \tag{12}$$

Here, $g_{\rm on}$ and $g_{\rm off}$ are the conductances of the ion-conducting state (C_4) and nonconducting state, respectively. So, we set $g_{\rm off} = 0$ and $g_{\rm on} = g$; the latter generally depends on the external voltage, $V(t)$. V_r denotes the resting potential of the channel molecule. Equation (12) then reduces to

$$I(t) = G(P_4, V(t), t)(V(t) - V_r), \tag{13}$$

where $G(P_4, V(t), t) = g(V(t))P_4(t)$ is the memory conductance or memductance of the ion channel.[38,39] Equations (6) and (13) construct the system of memristive equations of the ion channel. We point out that, even if the conductance g is a constant, the ion channel can exhibit memory effects due to the voltage dependence of $P_4(t)$ that will lead to a nonlinear relationship between integrals of current and voltage.[40] The memory, however, is dynamic and disappears when the voltage is kept fixed.

IV. STOCHASTIC THERMODYNAMICS OF THE ION CHANNEL

The internal energy U and entropy S of a system at time t are defined in terms of the probability of the system to be in state-m, $P_m(t)$, as[41–43]

$$U(t) = -T' \sum_m P_m(t) \ln P^{\rm st}_m(V_t)$$

and

$$S(t) = -\sum_m P_m(t) \ln P_m(t), \tag{14}$$

where we set the Boltzmann constant, $k_B = 1$. $P^{\rm st}_m(V_t)$ is the stationary probability the system would have if the driving voltage was frozen at time t at the value V_t.[44] The free energy of the system is then given by

$$F(t) = U(t) - T'S(t) = T' \sum_m P_m(t) \ln \frac{P_m(t)}{P^{\rm st}_m(V_t)}. \tag{15}$$

From Eqs. (3) and (14), the system EPR becomes[45]

$$\dot{S}(t) = \sum_{m,m'} W_{m',m}(V(t))P_{m'}(t) \ln \frac{P_{m'}(t)}{P_m(t)} \tag{16}$$

that can be split as[46,47]

$$\dot{\rm S}({\rm t}) = \dot{\rm S}_{\rm tot}({\rm t}) - \dot{\rm S}_{\rm m}({\rm t}). \tag{17}$$

Here, the first term in the rhs of Eq. (17) gives the total EPR characterizing the dissipation and the second term denotes the medium EPR due to the entropy flow into the surroundings (which is assumed to be ideal, *i.e.*, no entropy production of its own[45]). Their expressions are as follows:

$$\begin{aligned} \dot{S}_{tot}(t) &= \sum_{m,m'} W_{m',m}(V(t))P_{m'}(t) \ln \frac{W_{m',m}P_{m'}(t)}{W_{m,m'}P_m(t)}, \\ \dot{S}_m(t) &= \sum_{m,m'} W_{m',m}(V(t))P_{m'}(t) \ln \frac{W_{m',m}}{W_{m,m'}}. \end{aligned} \tag{18}$$

There is another division of the total EPR into adiabatic and nonadiabatic contributions. This is highly relevant for the system under consideration with time-dependent external driving that breaks the detailed balance.[44] The adiabatic and nonadiabatic EPRs are defined as[44,45]

$$\dot{S}_a(t) = \sum_{m,m'} W_{m',m}(V(t))P_{m'}(t) \ln \frac{W_{m',m}P^{\rm st}_{m'}(V_t)}{W_{m,m'}P^{\rm st}_m(V_t)} \tag{19}$$

and

$$\dot{S}_{na}(t) = \sum_{m,m'} W_{m',m}(V(t))P_{m'}(t) \ln \frac{P_{m'}(t)P^{\rm st}_m(V_t)}{P_m(t)P^{\rm st}_{m'}(V_t)}. \tag{20}$$

When the driving is infinitely slow, one is in the adiabatic limit. The system at all times remains virtually in steady state with $P^{\rm ss}_m(t) \to P^{\rm st}_m(V_t)$ and the nonadiabatic contribution to the total EPR goes to zero (see Eq. (20)). For a finite rate of driving, there is non-zero nonadiabaticity.

To appreciate the utility of this division, we consider the situation at some specific time t. If the voltage was fixed at say, V_t, that obviously depends on the value of t, then the system properties would depend on the voltage *parametrically*. In this case, with the initial condition chosen as the channel being in the state C_0, the time-dependent solution of Eq. (3) is given by a binomial distribution of the form[34]

$$P_m(t) = \binom{n_T}{m} (B(t))^m (1 - B(t))^{n_T - m}, \tag{21}$$

where

$$B(t) = \frac{k_1(V_t)(1 - \exp(-(k_1(V_t) + k_{-1}(V_t))t))}{k_1(V_t) + k_{-1}(V_t)}. \tag{22}$$

Then, the stationary solution is

$$P^{\rm st}_m(V_t) = \binom{n_T}{m} (B^{\rm st})^m (1 - B^{\rm st})^{n_T - m} \tag{23}$$

with

$$B^{\rm st} = \frac{k_1(V_t)}{k_1(V_t) + k_{-1}(V_t)}. \tag{24}$$

The explicit expression of total EPR at time t is given by

$$\dot{S}_{tot}(t) = J(t) \ln \left(\frac{k_1(V_t)(1 - B(t))}{k_{-1}(V_t)B(t)} \right). \tag{25}$$

Here, $J(t)$ is the net flux[45] defined as

$$\begin{aligned} J(t) &= \sum_{m,m'} J_{m',m}(t) \\ &= \sum_{m,m'} W_{m',m}(V_t)P_{m'}(t) - W_{m,m'}(V_t)P_m(t) \\ &= k_1(V_t)n_T(1 - B(t)) - k_{-1}(V_t)n_T B(t). \end{aligned} \tag{26}$$

Now, at stationary state, putting Eq. (24) into Eq. (26), we get

$$J^{\rm st} = 0 = \dot{S}^{\rm st}_{tot} = \dot{S}^{\rm st}_a = \dot{S}^{\rm st}_{na}. \tag{27}$$

Thus, if the voltage was kept fixed at V_t, the ion channel would reach thermodynamic equilibrium, satisfying the detailed balance condition

$$J^{\rm st}_{m',m} = W_{m',m}(V_t)P^{\rm st}_{m'}(V_t) - W_{m,m'}(V_t)P^{\rm st}_m(V_t) = 0. \tag{28}$$

Now, with the help of Eq. (28), it is easy to see from Eq. (19) that, *even when the voltage is time-dependent*, $\dot{S}_a(t)$

$= 0\ \forall t$. However, in presence of time-varying voltage, the fluxes in the long-time limit, defined in terms of the probabilities $P_m^{\rm ss}(t)$, are non-zero as

$$J^{\rm ss}_{m',m}(t) = W_{m',m}(V(t))P^{\rm ss}_{m'}(V(t)) - W_{m,m'}(V(t)) \times P^{\rm ss}_m(V(t)) \neq 0. \tag{29}$$

The system then has a non-zero dissipation $\dot{S}^{\rm ss}_{tot}(t) = \dot{S}^{\rm ss}_{na}(t) > 0$. Thus, the total EPR of the ion channel comes entirely from the nonadiabatic contribution arising due to external driving. Before proceeding further, we express $\dot{S}_{na}(t)$ in a more compact form[45]

$$\begin{aligned}\dot{S}_{na}(t) &= \sum_m \ln \frac{P^{\rm st}_m(V_t)}{P_m(t)} \sum_{m'} W_{m',m}P_{m'}(t) \\ &\quad + \sum_{m'} P_{m'}(t) \ln \frac{P_{m'}(t)}{P^{\rm st}_{m'}(V_t)} \sum_m W_{m',m} \\ &= -\sum_m \dot{P}_m(t) \ln \frac{P_m(t)}{P^{\rm st}_m(V_t)}.\end{aligned} \tag{30}$$

The final expression is obtained using Eqs. (3) and (4).

From Eq. (15), the rate of free energy change can be written as

$$\begin{aligned}\frac{\dot{F}(t)}{T'} &= \sum_m \left(\dot{P}_m \ln P_m + \dot{P}_m - \dot{P}_m \ln P^{\rm st}_m - P_m(t)\frac{\dot{P}^{\rm st}_m}{P^{\rm st}_m}\right) \\ &= \sum_m \left(\dot{P}_m \ln \frac{P_m}{P^{\rm st}_m} - P_m(t)\frac{\dot{P}^{\rm st}_m}{P^{\rm st}_m}\right), \text{ as } \sum_m \dot{P}_m = 0 \\ &= -\dot{S}_{na}(t) - \sum_m P_m(t)\frac{\dot{P}^{\rm st}_m}{P^{\rm st}_m}.\end{aligned} \tag{31}$$

The last line follows from Eq. (30). Now, following Esposito and Van den Broeck,[45] the nonadiabatic EPR can be split into "boundary" and "driving" contributions as

$$\dot{S}_{na}(t) = \dot{S}_b(t) + \dot{S}_d(t), \tag{32}$$

where

$$\begin{aligned}S_b(t) &= -\sum_m P_m(t) \ln \frac{P_m(t)}{P^{\rm st}_m(V_t)} = -\frac{F(t)}{T'}, \\ \dot{S}_d(t) &= -\sum_m P_m(t)\frac{\dot{P}^{\rm st}_m(V_t)}{P^{\rm st}_m(V_t)}.\end{aligned} \tag{33}$$

Using Eqs. (32) and (33), one obtains

$$\frac{\dot{F}(t)}{T'} = -\dot{S}_b(t) = -\dot{S}_{na}(t) + \dot{S}_d(t). \tag{34}$$

From the Eqs. (15), (17), and (34), we get

$$\dot{U}(t) = T'(\dot{S}_a(t) - \dot{S}_m(t) + \dot{S}_d(t)).$$

Defining $h_d(t) = T'\dot{S}_m(t)$ as the heat dissipation rate to the surroundings and $w_d(t) = T'\dot{S}_d(t)$ as the rate of dissipative work done on the ion channel by the external voltage, one can write down a first-law like expression,[43]

$$\dot{U}(t) + h_d(t) = w_d(t), \tag{35}$$

where $\dot{S}_a(t) = 0$, as already mentioned. Here, we provide an analytical expression of w_d for the ion channel. From Eq. (23), we have

$$\dot{P}^{\rm st}_m(V_t) = \frac{Q\dot{V}(t)}{k_BT'}P^{\rm st}_m(V_t)\left[m - \frac{n_T}{1+z}\right], \tag{36}$$

where $z = \frac{k_{-1}(0)}{k_1(0)}\exp(-QV(t)/k_BT')$ and $Q = q_+ - q_-$. Then, using Eq. (33), we get

$$w_d(t) = T'\dot{S}_d(t) = -T'\sum_m P_m(t)\frac{Q\dot{V}(t)}{k_BT'}\left[m - \frac{n_T}{1+z}\right]. \tag{37}$$

Next, we treat some specific cases.

A. Adiabatic driving

In the adiabatic limit of the voltage variation, we take its frequency $\omega \to 0$. As the ion channel attains equilibrium for a fixed voltage ($\omega = 0$), so the case of infinitely slowly varying voltage should also give the same result in the long-time limit. This is easy to verify using the fact that in the $\omega \to 0$ limit, $P^{\rm ss}_m(t) \to P^{\rm st}_m(V_t)$. Then, from Eq. (20) (or Eq. (30)),

$$\dot{S}^{\rm ss}_{na}(t) = 0 = \dot{S}^{\rm ss}_{tot}(t) \tag{38}$$

as $\dot{S}_a(t) = 0, \forall t$. So, for adiabatic driving, the ion channel indeed reaches equilibrium. Also, when $P^{\rm ss}_m(t) \to P^{\rm st}_m(V_t)$, detailed balance is satisfied resulting in zero flux and then $\dot{S}^{\rm ss}(t) = \dot{S}^{\rm ss}_m(t) = 0$. Finally, from Eqs. (32), (33), and (35), one obtains $\dot{S}^{\rm ss}_b(t) = 0 = \dot{F}^{\rm ss}(t) = \dot{S}^{\rm ss}_d(t) = \dot{U}^{\rm ss}(t)$.

B. Extreme nonadiabatic driving

Extreme nonadiabatic driving indicates the $\omega \to \infty$ limit. For $\frac{k_1(0)}{k_{-1}(0)} \gg 1$, the ion-conducting state probability $P^{\rm ss}_4(t)$ dominates with $P^{\rm ss}_0(t)$, $P^{\rm ss}_1(t)$, $P^{\rm ss}_2(t)$ being negligibly small.[27] Then, from Eq. (20), we can write approximately

$$\begin{aligned}\dot{S}^{ss}_{na}(t) &\approx \left[k_1(t)(1 - P^{ss}_4(t)) - n_Tk_{-1}(t)P^{ss}_4(t)\right] \\ &\quad \times \ln \frac{P^{\rm st}_4(V_t)(1 - P^{ss}_4(t))}{P^{\rm st}_3(V_t)P^{ss}_4(t)}.\end{aligned} \tag{39}$$

Using Eq. (23), we get

$$\frac{P^{\rm st}_4(V_t)}{P^{\rm st}_3(V_t)} = \frac{k_1(t)}{n_Tk_{-1}(t)}. \tag{40}$$

Also, from Eq. (11),

$$P^{\rm ss}_4 = \frac{\langle\kappa(t)\rangle}{\langle K(t)\rangle} \approx \frac{\langle k_1(t)\rangle}{\langle K(t)\rangle}. \tag{41}$$

Putting Eqs. (40) and (41) into Eq. (39), one has

$$\dot{S}^{ss}_{na}(t) \approx J_f(t) \ln \frac{k_1(t)\langle k_{-1}(t)\rangle}{k_{-1}(t)\langle k_1(t)\rangle} = \dot{S}^{ss}_{tot}(t), \tag{42}$$

where

$$J_f(t) = n_T\left[\frac{k_1(t)\langle k_{-1}(t)\rangle - k_{-1}(t)\langle k_1(t)\rangle}{\langle K(t)\rangle}\right]. \tag{43}$$

Here, $\langle k_{\pm1}(t)\rangle = f_\pm k_{\pm1}(0)$ with $f_\pm = \langle\exp(q_\pm V(t)/k_BT')\rangle$. It is straight-forward to derive the system and medium EPRs as

$$\dot{S}^{ss}(t) \approx J_f(t) \ln \frac{\langle k_{-1}(t)\rangle}{\langle k_1(t)\rangle}, \quad \dot{S}^{ss}_m(t) \approx J_f(t) \ln \frac{k_1(t)}{k_{-1}(t)}. \tag{44}$$

Now, as $P_0^{ss}(t)$, $P_1^{ss}(t)$, $P_2^{ss}(t)$ are insignificant in the $\omega \to \infty$ limit, from Eq. (37), we get

$$\dot{S}_d^{ss}(t) = w_d^{ss}(t)/T' = -\frac{Q\,\dot{V}(t)}{k_B T'}\left[P_4^{ss} + \frac{3z-1}{1+z}\right], \quad (45)$$

where z is defined as in Eq. (36).

If one takes $q_+ = -q_- = q$, one gets $f_+ = f_-$ and $Q = 2q$ in this symmetric case. Then, P_4^{ss} reduces to $P_4^{ss} = \frac{k_1(0)}{k_1(0)+n_T k_{-1}(0)}$ and we have

$$\dot{S}_{na}^{ss}(t) \approx 4n_T P_4^{ss} k_{-1}(0)\sinh(xV(t))xV(t) = \dot{S}_{tot}^{ss}(t), \quad (46)$$

where $x = q/k_B T'$. Also, from Eq. (45), one can write in this case,

$$\dot{S}_d^{ss}(t) = -2x\dot{V}(t)\left[P_4^{ss} + \frac{3z-1}{1+z}\right]. \quad (47)$$

Then, from Eqs. (34) and (35), respectively, one obtains

$$\begin{aligned}\dot{S}_b^{ss}(t) &= -\dot{F}^{ss}(t)/T' = \dot{S}_{na}^{ss}(t) - \dot{S}_d^{ss}(t)\\ &= 2xP_4^{ss}\left[2n_T k_{-1}(0)\sinh(xV(t))V(t) + \dot{V}(t)\right]\\ &\quad + 2x\dot{V}(t)\left(\frac{3z-1}{1+z}\right) \quad (48)\end{aligned}$$

and

$$\begin{aligned}\dot{U}^{ss}(t)/T' &= \dot{S}_d^{ss}(t) - \dot{S}_m^{ss}(t)\\ &= 2P_4^{ss}\left[n_T k_{-1}(0)\sinh(xV(t))\ln z(t) - x\dot{V}(t)\right]\\ &\quad - 2x\dot{V}(t)\left(\frac{3z-1}{1+z}\right). \quad (49)\end{aligned}$$

C. Thermodynamic quantities per cycle

For periodic external voltage, in the long-time limit, the response of the system also becomes periodic with the same time period. As internal energy, entropy, and free energy of the system are all state functions, their change over a time period T of the external voltage will be zero, *i.e.*, $\Delta X^c = \int_0^T \dot{X}(t)dt = 0$, where $X \equiv U, S, F$ (and S_b) with superscript "c" indicating change of X over a cycle. Then, we have

$$\Delta S_{tot}^c = \Delta S_m^c = \Delta S_{na}^c = \Delta S_d^c. \quad (50)$$

So, the total dissipation of the ion channel per cycle in the long-time limit is equal to the heat dissipation to the environment, and this is generated solely by the driving part of the nonadiabatic entropy production.

V. TEMPORAL SYMMETRY AND HYSTERESIS

Application of periodic external voltage on the ion channel can develop memory effect in the system which is manifested in terms of the hysteresis in the current($I(t)$)-voltage($V(t)$) plots. This effect is prominent when the time scales of the external voltage and system's natural relaxation match and tend to vanish at voltage frequencies too low and too high, representing adiabatic and extreme nonadiabatic drivings, respectively. Here, we analyze the hysteresis in different thermodynamic functions of the ion channel, along with the current, in these two limiting conditions. Specifically, we investigate the symmetry properties of the system's different periodic responses with respect to time over a cycle. All the analytical treatments are performed in the long-time limit using the closed-form expressions of $P_4^{ss}(t)$ given in Eq. (11). For intermediate frequencies of the external voltage, detailed numerical analyses of hysteresis will be done in Sec. VI.

At first, we study the $\omega \to 0$ limit. In this case, all the thermodynamic functions discussed here are zero in the $t \to \infty$ limit and the system virtually attains equilibrium as already discussed in Sec. IV. So, we concentrate on the ionic current given in Eq. (13). From the expression of the periodic voltage, $V(t) = V_a \sin\omega t$, one can write

$$\begin{aligned}V(t) &= V(T/2 - t) = -V(t - T/2),\\ V(t + T/2) &= V(T - t) = -V(t).\end{aligned}$$

For $\omega \to 0$, we have from Eq. (11), $P_4^{ss}(t) = \frac{\kappa(t)}{K(t)}$ and then, from Eq. (13), over a period, the following symmetry relations hold with $0 \le t \le T/2$:

$$\begin{aligned}&I(t) = I(T/2 - t), \quad \text{positive half-cycle of } V(t),\\ &I(t + T/2) = I(T - t), \quad \text{negative half-cycle of } V(t).\end{aligned} \quad (51)$$

It follows from Eq. (51) that, over the positive as well as the negative half-cycle of the voltage, the current retraces its path and there is *no scope of hysteresis in the $I - V$ curve*. We point out that this temporal symmetry is valid individually for positive and negative half-cycles but these two regions are not generally connected by symmetry as

$$I(t) \ne I(t + T/2), \forall t \ne 0. \quad (52)$$

Next, we come to the $\omega \to \infty$ limit where P_4^{ss} becomes time-independent. Then, the same temporal symmetry relations are valid for the ionic current as given in Eq. (51) above. But, in this limit, the system is far away from equilibrium with significant dissipation. This is a bit counter-intuitive as vanishing hysteresis indicates vanishing dissipation. Thus, we explore the hysteresis in other properties of the system.

Let us take the dissipation function $\dot{S}_{tot}^{ss}(t) = \dot{S}_{na}^{ss}(t)$. From Eq. (42), with symmetry of $V(t)$ given above, we have the same symmetry as of the ionic current,

$$\begin{aligned}&\dot{S}_{tot}^{ss}(t) = \dot{S}_{tot}^{ss}(T/2 - t), \quad \text{positive half-cycle of } V(t),\\ &\dot{S}_{tot}^{ss}(t + T/2) = \dot{S}_{tot}^{ss}(T - t), \quad \text{negative half-cycle of } V(t),\end{aligned} \quad (53)$$

and also the asymmetry $\dot{S}_{tot}^{ss}(t) \ne \dot{S}_{tot}^{ss}(t + T/2)$, $\forall t \ne 0$. So the $\dot{S}_{tot}^{ss} - V$ curve also becomes hysteresis-less. Interestingly, in the symmetric case of $q_+ = -q_- = q$, the asymmetry also disappears and one finds from Eq. (46) that

$$\dot{S}_{tot}^{ss}(t) = \dot{S}_{tot}^{ss}(t + T/2)\,\forall t. \quad (54)$$

Hence, *the period of the dissipation function becomes half of that of the external voltage in the symmetric case in the high-frequency limit.*[27] It is easy to see that, even in this case, the ionic current does not have this symmetry. One can easily verify that the same temporal symmetry relations given in Eq. (53) are valid for $\dot{S}^{ss}(t)$ and $\dot{S}_m^{ss}(t)$ (see Eq. (44)) but not the symmetry of Eq. (54).

Next, we come to the case of $\dot{S}_d^{ss}(t)$. We have the following temporal symmetries:

$$\dot{V}(T/2-t) = -\dot{V}(t),\ \dot{V}(t+T/2) = -\dot{V}(T-t) = -\dot{V}(t),$$
$$z(T/2-t) = z(t),\ z(t+T/2) = z(T-t),$$

where z is defined as in Eq. (45). Using these relations, we find from Eq. (45)

$$\begin{aligned}\dot{S}_d^{ss}(t) &= -\dot{S}_d^{ss}(T/2-t), \quad \text{positive half-cycle of } V(t),\\ \dot{S}_d^{ss}(t+T/2) &= -\dot{S}_d^{ss}(T-t), \quad \text{negative half-cycle of } V(t).\end{aligned} \tag{55}$$

Hence, $\dot{S}_d^{ss}(t)$ (and w_d) is actually *antisymmetric* over the voltage half-cycles; rather than retracing its path, the curve of $\dot{S}_d^{ss}(t) - V(t)$ over $0 \le t \le T/4$ is farthest from that over $T/4 \le t \le T/2$ and the same thing occurs for the next two quarters. This clearly suggests that the $\dot{S}_d^{ss}(t) - V(t)$ curve contains a finite amount of hysteresis. As these results are in the $\omega \to \infty$ limit, so the hysteresis has no scope to disappear and we speculate that the amount of hysteresis actually grows with ω. In Sec. VI, we will investigate the system numerically in the intermediate frequency range to verify this point. But, it is evident that *not all the plots of thermodynamic functions versus voltage are devoid of hysteresis, even in the high-frequency limit*. This feature justifies the maximum average dissipation in this limit where the system resides arbitrarily away from equilibrium. It is obvious that the symmetry relations remain valid for $q_+ = -q_- = q$ (see Eq. (47)).

A close look at Eq. (34) reveals that the evolution of $\dot{S}_b^{ss}(t)$ over a period occurs in such a way that $\dot{S}_{na}^{ss}(t) - V(t)$ curve contains no hysteresis. Now, analyzing Eq. (48), where $q_+ = -q_- = q$, we find that the above mentioned temporal symmetries are absent in the evolution of $\dot{S}_b^{ss}(t)$ over a period except the trivial fact that it is periodic. Hence, the plot of $\dot{S}_b^{ss}(t) - V(t)$ must also accommodate hysteresis. As even the symmetric case of $q_+ = -q_- = q$ cannot prevent hysteresis, in the general case of $q_+ \neq -q_-$, hysteresis will prevail certainly. According to Eq. (34), this feature is identically reflected in the rate of free energy change of the ion channel. From Eq. (49), one can also find out that the same feature is present in the $\dot{U}^{ss}(t) - V(t)$ plot. We summarize the temporal symmetry and the fate of hysteresis of different quantities in Table I in the high-frequency limit.

Before progressing to the numerical analyses, here, we briefly mention the possible experimental detection of the hysteresis behavior, particularly the growing hysteresis in some thermodynamic functions, *e.g.*, in $\dot{S}_d^{ss}(t)$. It follows from Eq. (45) that, a knowledge of P_4^{ss} along with the other system parameters like the rate constants, gating charge is essential to determine the quantity. Now, it is standard practice to determine the ion channel current and fit the data to some relevant scheme, by employing optimization techniques such as simulated annealing for a given input voltage protocol,[21] to get those parameters along with the conducting (or open) state probability.[22] Thus, one can then calculate the thermodynamic functions from our theoretical relations and verify the nature of hysteresis. In Sec. VI, we will analyze the behavior of various functions numerically using such experimentally obtained model parameters. Of course, this is not a direct measurement scheme. Calorimetric measurements can detect the heat dissipation, but it is related to the medium entropy production rate $\dot{S}_m^{ss}(t)$ that shows no hysteresis in the high-frequency limit. *Although difficult, this feature, in principle, can be directly tested and act as a support of the theory.*

In connection to experimental measurement, it is also important to mention the role of the lipid bilayer, in which the ion channel is reconstituted, in governing the structure and function of the latter.[48–50] The lipid-protein interactions, *e.g.*, between the lipid head-groups and protein side-chains, have been shown to be very important in the gating mechanism. *However, the interaction dynamics are very hard to characterize and not much data are available*.[49] The results presented here, then, may act as a reference for experimentalists to judge the non-ideality introduced due to the lipid environment over the frequency range of the external voltage. Of course, extending the model system to include the effect of lipid bilayer will require further experimental support and is beyond the scope of the present work.

VI. NUMERICAL RESULTS

We numerically solve Eq. (3) using the Heun's algorithm (step size of 10^{-6} s) with the following parameter values: $k_1(0) = 125.0\ \text{s}^{-1}$, $k_{-1}(0) = 5.0\ \text{s}^{-1}$, $q_+ = q_- = 0.7\text{e}$, $V_r = -90$ mV, and $V_a = 45$ mV. These are taken following the experimental results and the corresponding data of Kargol *et al.*[22] The temperature is set at $T' = 285$ K and we take a constant conduc-

TABLE I. Temporal symmetry and hysteretic behavior of ionic current $I(t)$ and various thermodynamic functions over a period T in the high-frequency limit. The loop area of the plot of some function against the external voltage $V(t)$ is a measure of hysteresis regarding that function.

Quantity	Temporal symmetry	Hysteresis
$I(t)$	Symmetric over +ve and −ve half-cycle	Vanish
$\dot{S}^{ss}(t)$	Symmetric over +ve and −ve half-cycle	Vanish
	Antisymmetric around $T/2$ for $q_+ = -q_- = q$	
$h_d^{ss}(t) = T'\dot{S}_m^{ss}(t)$	Symmetric over +ve and −ve half-cycle	Vanish
$\dot{S}_{tot}^{ss}(t) = \dot{S}_{na}^{ss}(t)$	Symmetric over +ve and −ve half-cycle	Vanish
	Symmetric around $T/2$ for $q_+ = -q_- = q$	
$w_d^{ss}(t) = T'\dot{S}_d^{ss}(t)$	Antisymmetric over +ve and −ve half-cycle	Finite
$\dot{U}^{ss}(t)$	Asymmetric over +ve and −ve half-cycle	Finite
$\dot{F}^{ss}(t) = -T'\dot{S}_b^{ss}(t)$	Asymmetric over +ve and −ve half-cycle	Finite

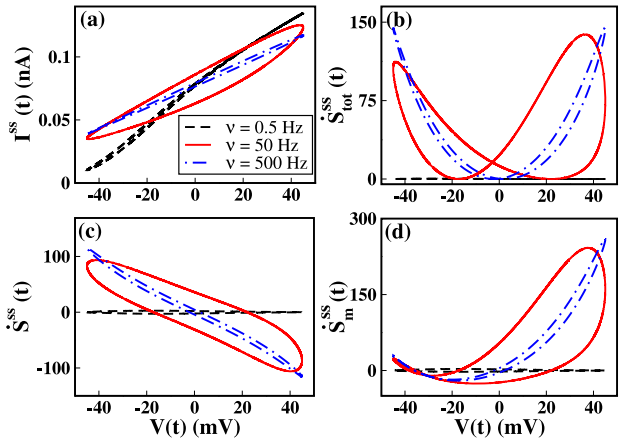

FIG. 1. Dynamic hysteresis in the long-time limit in (a) ionic current, $I^{ss}(t)$, (b) total EPR, $\dot{S}^{ss}_{tot}(t)$, (c) system EPR, $\dot{S}^{ss}(t)$, and (d) medium EPR, $\dot{S}^{ss}_{m}(t)$. The loops are generated by plotting data over a period T.

tance $g = 0.001\ \mu$S. We thoroughly analyze the conducting-state probability $P_4(t)$, the ionic current $I(t)$, and various EPRs as a function of frequency ν of the external voltage $V(t)$. The details of their behavior, particularly the dynamic hysteresis, are already discussed elsewhere.[27] However, for the sake of completeness and readability, we provide some representative plots here in the long-time limit.

In Fig. 1, we show the dynamic nature of the hysteresis in the current $I^{ss}(t)$ as well as in different EPRs by taking voltage frequencies over a large range. It is evident from the figure that, in the low ($\nu = 0.5$ Hz) and high ($\nu = 500$ Hz) frequency situations, the hysteresis, measured in terms of the loop area, tends to disappear for all the quantities. This is further emphasized in Fig. 2(a), where we plot the $I - V$ loop area, normalised by the maximum value, as a function of ν. The curve passes through a maximum and tends to zero in the two limiting situations. However, the average (over a period T) total EPR, $\langle \dot{S}^{ss}_{tot}(t) \rangle$ rises with ν to saturation as shown in Fig. 2(b).

Next, we study the time-evolutions of $w^{ss}_d(t)$, $\dot{F}^{ss}(t)$, and $\dot{U}^{ss}(t)$, all scaled by temperature T', at a high frequency $\nu = 5000$ Hz, at a low frequency $\nu = 0.5$ Hz, and also at an intermediate frequency $\nu = 50$ Hz. The corresponding plots are given in Figs. 3(a)–3(c), respectively, over a period. In the high-frequency limit, all three quantities show the same dynamics, manifested in Fig. 3(a). This follows from the fact that at large ν (or ω), they are dominated by and proportional to ω coming from the $\dot{V}$ term (see Eqs. (45) and (47)–(49)). We have also shown the accuracy of the analytical treatment in the $\omega \to \infty$ limit by plotting points generated from Eq. (47). Closer inspection of these plots also reveals the temporal symmetry mentioned in Table I. We clarify here that, although $\dot{F}^{ss}(t)$ and $\dot{U}^{ss}(t)$ are supposed to be asymmetric over the positive and negative half-cycles, the terms causing this asymmetry *do not* contain $\dot{V}$ (see Eqs. (48) and (49)). Thus, they become negligible in the high-frequency limit and the corresponding dynamics becomes *antisymmetric*, similar to that of $w^{ss}_d(t)$. High values of ν are also shown to be experimentally accessible, *e.g.*, in Ref. 22, ν is varied in the range 100 Hz-4 kHz.

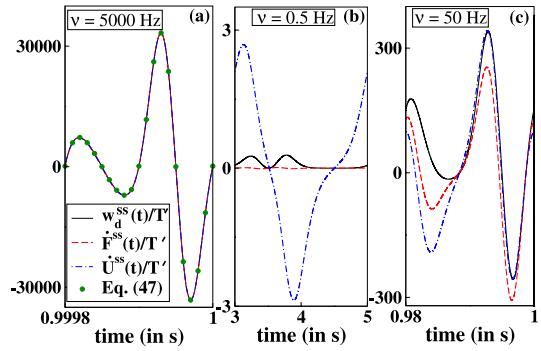

FIG. 3. Dynamics of $w^{ss}_d(t)/T'$, $\dot{F}^{ss}(t)/T'$, and $\dot{U}^{ss}(t)/T'$ over a period for (a) $\nu = 5000$ Hz, (b) $\nu = 0.5$ Hz, and (c) $\nu = 50$ Hz.

Now, we come to the corresponding hysteresis plots of these thermodynamic functions which is the point of main attention. In Fig. 4(a), the low frequency case $\nu = 0.5$ Hz is shown. All the quantities have small amount of hysteresis with the loop area of $\dot{U}^{ss}(t) - V(t)$ being much larger compared to that of the others. Interestingly, as ν is increased, the hysteresis becomes more and more prominent. This is evident from Figs. 4(b)-4(d), where the loops for $\dot{U}^{ss}(t)$, $w^{ss}_d(t)$, and $\dot{F}^{ss}(t)$, respectively, are found to expand progressively with increasing ν. It is observed from Fig. 4 that the magnitudes of $\dot{U}^{ss}(t)/T', w^{ss}_d(t)/T'$, and $\dot{F}^{ss}(t)/T'$ in the negative V(t) region are larger than those in the positive V(t) region regardless

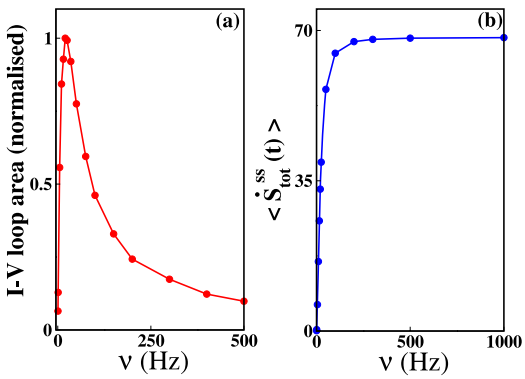

FIG. 2. (a) Normalised $I - V$ loop area and (b) average total EPR, $\langle \dot{S}^{ss}_{tot}(t) \rangle$ as a function of ν.

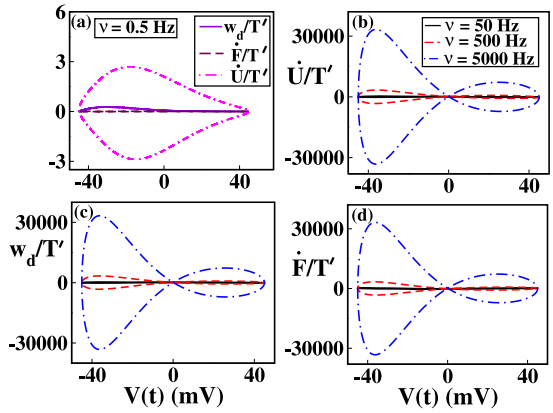

FIG. 4. (a) Hysteresis loops of $w^{ss}_d(t)/T'$, $\dot{F}^{ss}(t)/T'$, and $\dot{U}^{ss}(t)/T'$ over a period at $\nu = 0.5$ Hz. The hysteresis loops of $\dot{U}^{ss}(t)/T'$, $w^{ss}_d(t)/T'$, and $\dot{F}^{ss}(t)/T'$ are shown in (b)-(d), respectively, at $\nu = 50$, 500, 5000 Hz.

of the frequency. This can be explained analytically in the high-frequency limit. All the three quantities are dominated by the $\dot{V}$ containing terms at large ν, as already stated above. Now, the factor $(\frac{3z-1}{1+z})$ is large when $V(t) < 0$ (see Eq. (36) for the definition of z) and this results in the higher magnitude in negative $V(t)$ region. This is valid also for intermediate frequencies as obtained numerically. The result suggests different nonequilibrium thermodynamic responses of the ion channel molecule to depolarization and repolarization steps of the periodic voltage. Thus, these specific thermodynamic functions exhibit an entirely different feature of ever-growing hysteresis in presence of external periodic voltage. We conjecture that this increasing hysteresis actually reflects the *lasting* memory of the ion channel in far-from-equilibrium scenarios. For clarity, we mention that this memory exists as long as the voltage variation is present.

VII. SUMMARY AND CONCLUSION

In this work, we have studied the stochastic kinetics of a single K^+ channel in presence of external periodic voltage. The time-dependent driving keeps the system out-of-equilibrium characterized by positive dissipation. The appealing aspect of the system's response is the dynamic hysteresis shown by the experimentally measurable ionic current as well as various EPRs. This reveals the memory of the channel molecule generated due to the sinusoidal driving. Although hysteresis in diverse properties has been found to vanish in the low as well as in the high-frequency limit, here, we show that this is *not* universally true. From the temporal symmetry of the evolution in the high-frequency limit and detailed numerical study, we have established that for some thermodynamic functions, *viz.*, the rates of internal energy and free energy changes of the system and the rate of dissipative work done on the system, the hysteresis actually grows with rising voltage frequency. The temporal symmetry analysis also allows one to analytically determine whether hysteresis will emerge without going into the more involved loop-area calculations and provides a tangible qualitative understanding of the development and sustenance of memory. The growing hysteresis also corroborates with the non-zero average dissipation. Therefore, we propose that the memory of the ion channel resulting due to periodic voltage *is not reflected uniformly in all of its properties*. Most importantly, the detectable ionic current gives an impression of continuous attenuation of memory as voltage variation becomes faster. However, the memory effect, although dynamic, actually flourishes with rising frequency as exhibited through specific nonequilibrium thermodynamic responses. It will be highly interesting to quantitatively examine the dynamic hysteresis in these functions employing more realistic models, including interaction among the subunits and with the environment. Work in this direction is in progress.

ACKNOWLEDGMENTS

K.B. acknowledges Dr. B. Das, Professor G. Gangopadhyay, Professor K. Bhattacharyya, and Professor C. Mukhopadhyay for fruitful discussions and the University Grants Commission (UGC), India for Dr. D. S. Kothari Fellowship.

[1]A. L. Hodgkin and A. F. Huxley, J. Physiol. **117**, 500 (1952).
[2]D. L. Nelson and M. M. Cox, *Lehninger Principles of Biochemistry*, 4th ed. (Worth, 2004).
[3]R. F. Fox and Y. Lu, Phys. Rev. E **49**, 3421 (1993).
[4]F. Bezanilla, IEEE Trans. Nanobioscience **4**, 34 (2005).
[5]Y. Pichon, L. Prime, P. Benquet, and F. Tiaho, Eur. Biophys. J. **33**, 211 (2004).
[6]G. M. Shepherd, *Neurobiology*, 3rd ed. (Oxford University Press, New York, Oxford).
[7]W. N. Zagotta, T. Hoshi, and R. W. Aldrich, J. Gen. Physiol. **103**, 321 (1994).
[8]W. N. Zagotta, T. Hoshl, J. Dittman, and R. W. Aldrich, J. Gen. Physiol. **103**, 279 (1994).
[9]T. Hoshi, W. N. Zagotta, and R. W. Aldrich, J. Gen. Physiol. **103**, 249 (1994).
[10]B. Sakmann and E. Neher, *Single-Channel Recording*, 2nd ed. (Plenum Press, New York, 1995).
[11]B. Hille, *Ion Channels of Excitable Membranes*, 3rd ed. (Sinauer Associates, Sunderland, MA, 2001).
[12]M. B. Jackson, B. S. Wong, C. E. Morris, and H. Lecar, Biophys. J. **42**, 109 (1983).
[13]L. Kaestner, P. Christophersen, I. Bernhardt, and P. Bennekou, Bioelectrochemistry **52**, 117 (2000).
[14]R. Mannikko, S. Pandey, H. P. Larsson, and F. Elinder, J. Gen. Physiol. **125**, 305 (2005).
[15]L. M. Nowak and J. M. Wright, Neuron **8**, 181 (1992).
[16]A. Fulinski, Z. Grzywna, I. Mellor, Z. Siwy, and P. N. R. Usherwood, Phys. Rev. E **58**, 919 (1998).
[17]H. Zhu, S. Dong, and J. M. Liu, Phys. Rev. B **70**, 132403 (2004).
[18]M. A. Pustovoit, A. M. Berezhkovskii, and S. M. Bezrukov, J. Chem. Phys. **125**, 194907 (2006).
[19]T. Andersson, Math. Biosci. **226**, 16 (2010).
[20]M. M. Millonas and D. A. Hanck, Phys. Rev. Lett. **80**, 401 (1998).
[21]M. M. Millonas and D. A. Hanck, Biophys. J. **74**, 210 (1998).
[22]A. Kargol, A. Hosein-Sooklal, L. Constantin, and M. Przestalski, Gen. Physiol. Biophys. **23**, 53 (2004).
[23]A. Kargol and K. Kabza, Phys. Biol. **5**, 026003 (2008).
[24]D. Fologea, E. Krueger, Y. I. Mazur, C. Stith, Y. Okuyama, R. Henry, and G. J. Salamo, Biochim. Biophys. Acta **1808**, 2933 (2011).
[25]J. P. Keener, J. Math. Biol. **58**, 447 (2009).
[26]B. K. Chakrabarty and M. Acharyya, Rev. Mod. Phys. **71**, 847 (1999).
[27]B. Das, K. Banerjee, and G. Gangopadhyay, Phys. Rev. E **86**, 061915 (2012).
[28]Y. Jiang, A. Lee, J. Chen, V. Ruta, M. Cadene, B. T. Chait, and R. MacKinnon, Nature **423**, 33 (2003).
[29]A. Nekouzadeh, J. R. Silva, and Y. Rudy, Biophys. J. **95**, 3510 (2008).
[30]L. M. Mannuzzu, M. M. Moronne, and E. Y. Isacoff, Science **271**, 213 (1996).
[31]W. R. Silverman, B. Roux, and D. M. Papazian, Proc. Natl. Acad. Sci. U. S. A. **100**, 2935 (2003).
[32]I. Goychuk and P. Hanggi, Physica A **325**, 9 (2003).
[33]D. Andrieux and P. Gaspard, J. Chem. Phys. **121**, 6167 (2004).
[34]B. Das and G. Gangopadhyay, J. Chem. Phys. **132**, 135102 (2010).
[35]K. Banerjee, B. Das, and G. Gangopadhyay, J. Chem. Phys. **138**, 165102 (2013).
[36]P. Gaspard, J. Chem. Phys. **120**, 8898 (2004).
[37]J. P. Keener, J. Math. Biol. **60**, 473 (2010).
[38]L. O. Chua and S. M. Kang, Proc. IEEE **64**, 209 (1976).
[39]L. O. Chua, IEEE Trans. Circuit Theory **18**, 507 (1971).
[40]D. B. Strukov, G. S. Snider, D. R. Stewart, and R. S. Williams, Nature (London) **453**, 80 (2008).
[41]L. Jiu-li, C. Van den Broeck, and G. Nicolis, Z. Phys. B **56**, 165 (1984).
[42]G. Nicolis and I. Prigogine, *Self-Organization in Nonequilibrium Systems* (Willey, New York, 1977).
[43]H. Ge and H. Qian, Phys. Rev. E **81**, 051133 (2010).
[44]M. Esposito and C. Van den Broeck, Phys. Rev. Lett. **104**, 090601 (2010).
[45]M. Esposito and C. Van den Broeck, Phys. Rev. E **82**, 011143 (2010).
[46]G. Nicolis and I. Prigogine, Proc. Natl. Acad. Sci. U. S. A. **68**, 2102 (1971).
[47]J. Schnakenberg, Rev. Mod. Phys. **48**, 571 (1976).
[48]T. S. Tillman and M. Cascio, Cell Biochem. Biophys. **38**, 161 (2003).
[49]A. W. Smith, Biochim. Biophys. Acta **1818**, 172 (2012).
[50]I. Basu, A. Chattopadhyay, and C. Mukhopadhyay, Biochim. Biophys. Acta **1838**, 328 (2014).